Journal of the Korean Physical Society, Vol. 60, No. 8, April 2012, pp. 1274∼1277

Tuning the Optical Orbital Angular Momentum of a Focused Gaussian Beam in an Optical Supperlattice under the Electro-optic Effect

Jie WANG, Jianhong SHI,* Linghao TIAN and Xianfeng CHEN†
Department of Physics, the State Key Laboratory on Fiber Optic Local Area Communication Networks and Advanced Optical Communication Systems, Shanghai Jiao Tong University, 800 Dong Chuan Road, Shanghai 200240, China

(Received 12 October 2011)

In this paper, we theoretically propose a new method to generate and tune the optical orbital angular momentum. A focused Gaussian beam passing through an optical superlattice under the electro-optic effect carries orbital angular momentum (OAM). This kind of OAM arises from the curl of the polarization. By adjusting the external electric field, the beam waist radius and the crystal length, we can obtain a dramatic variation of the OAM across the output light transverse section. This invention will find applications in the area of optical manipulation.

PACS numbers: 42.70.Mp, 42.30.Lr
Keywords: Angular momentum, Electro-optic effect, Gaussian beam
DOI: 10.3938/jkps.60.1274

I. INTRODUCTION

Nearly twenty years ago, Allen *et al.* [1] discovered that a light beam carries both orbital angular momentum (OAM) and spin angular momentum (SAM). The SAM is associated with circular polarizations of light, with each photon carrying $\pm\hbar$ angular momentum, depending on the handedness of the polarization. As is well known, the OAM arises from the spiral phase distribution at the wave-front of the light beam, described by $\exp(il\phi)$. Each photon carries an OAM of $l\hbar$. The OAM is decided by the spiral phase and can readily be generated using some linear techniques, *i.e.*, laser mode converters [2], spiral phase plates [3], computer generated holograms [4], and Pancharatnam-Berry phase optical elements [5], and some nonlinear methods [6]. Since Allen's discovery, as a natural character of light, OAM has drawn great attraction for its practical applications, such as nonlinear optics [7], optical tweezers [8], quantum information processing [9], and free space communications [10]. In recent decades, the applications of OAM have not been limited to visible light, but have been extended to other wave ranges, such as x-rays [11], sonic waves [12], and matter waves [13].

However, recent work has shown that OAM can also originate from the curl of the polarization [14]. In that experiment, a pair of orthogonal base vectors was employed to generate radial variant vector fields with hybrid states of polarizations (SOPs) that carries the OAM. *Tang et al.* [15] showed that for a focused Gaussian beam, a radial variant polarization in the transverse section of the beam could be formed while propagating in an optical superlattice under the electro-optic (EO) effect. Thus, this method can be used to generate and tune OAM.

In this paper, we theoretically analyze the behavior of the OAM of a focused Gaussian beam after passing through periodically-poled lithium niobate (PPLN) under the EO effect. We find that the OAM distribution of the light in the transverse section is related to the radius. Moreover, the OAM can be continually adjusted by changing the applied electric field, the waist radius and the crystal length.

II. THEORY AND SIMULATION

Due to the EO effect, the output beam of focused Gaussian light in PPLN can form a spatially radial varying polarization, which was first theoretically analyzed by Tang *et al.* [15]. Here, we use this method to generate and tune the OAM. Figure 1 shows the experimental setup for controlling the OAM in the output light section. An external electric field is applied along the y-axis, and a monochromatic light beam propagates in the x direction. The total field is expressed as follows [15]:

$$E(t) = E(0) + [E(r,x)\exp(-i\omega t)/2 + c.c.], \qquad (1)$$

where $E(0)$ is a dc electric or slowly varying electric field. Monochromic light with frequency ω can be depicted by

*E-mail: purewater@sjtu.edu.cn
†E-mail: xfchen@sjtu.edu.cn; Fax: 021-54747249

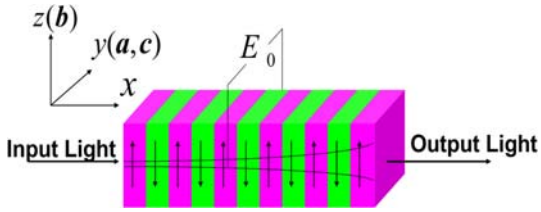

Fig. 1. (Color online) Schematic diagram for the generation of the OAM for a focused Gaussian beam in an optical superlattice (*e.g.*, a z-cut PPLN) under the electro-optic effect. A uniform electric field E_0 is applied along the y-axis of the PPLN sample. a and b are unit vectors of two independent electric field components. c is the direction of the applied electric field. The directions of the crystal domains are indicated by arrows.

$[E(r,x)\exp(-i\omega t)/2+c.c.]$, where $c.c.$ denotes the complex conjugate. Generally, $E(r,x)$ is considered as composition of two perpendicular vectors:

$$E(r,x) = E_1(r,x)\exp(ik_1x) + E_2(r,x)\exp(ik_2x), \quad (2)$$

Gaussian beams can be expressed as

$$E_j(r,x) = B_j(x)u_j(r,x)(j=1,2), \quad (3)$$

where $B_j(x)$ are the expansion coefficients of the Laguerre-Gauss modes of zero order, and $u_j(r,x)$ are the Gauss modes [16]. We focus the waist of a Gaussian beam on the input surface of the optical superlattice, and the waist radii W_j of E_j are equal ($W_j = W_0$), so the modes are given by

$$\begin{aligned} u_j(r,x) &= \sqrt{\frac{2}{\pi}}\frac{1}{W_0(1-i(2x/b_j))} \\ &\times \exp\left\{\frac{r^2}{W_0^2[1-i(2x/b_j)]}\right\}, \quad (4a) \\ B_1(x) &= \sqrt{\omega/n_1}g_1(x)a, \\ B_2(x) &= \sqrt{\omega/n_2}g_2(x)b, \quad E(0)=E_0c, \quad (4b) \end{aligned}$$

where the confocal parameters $b_j = k_jW_0^2$; a, b, and c are three unit vectors and $a\cdot b = 0$; $g_1(x)$ and $g_2(x)$ are the normalized amplitudes of the two independent wave components. When paraxial approximation holds, similarly to Ref. 17, the normalized amplitudes satisfy coupling equations as follows:

$$\begin{aligned} \frac{dg_1(x)}{dz} &= -id_1g_2(x)f_1\frac{1}{1+(x/b_1)^2(1-n_1/n_2)^2} \\ &\quad -id_2f(x)g_1(x), \quad (5a) \\ \frac{dg_2(x)}{dx} &= -id_3g_1(x)f_1\frac{1}{1+(x/b_1)^2(1-n_1/n_2)^2} \\ &\quad -id_4f(x)g_2(x), \quad (5b) \end{aligned}$$

with $d_1 = \frac{k_0}{2\sqrt{n_1n_2}}\gamma_{eff1}E_0$, $d_2 = \frac{k_0}{2n_1}\gamma_{eff2}E_0$, $d_3 = d_1$, $d_4 = \frac{k_0}{2n_2}\gamma_{eff3}E_0$, $f_1 = \frac{1}{L}\int_0^L f(x)\exp[iRx+\varphi(x)]\mathrm{dx}$, $\varphi(x) = \arg\{[1\pm i(x/b_1)(1-n_1/n_2)]^{-1}\}$, $f(x) = \mathrm{sgn}(\mathrm{Re}\{[1+i(x/b_1)(1-n_1/n_2)]^{-1}\exp(i\Delta kx)\})$, and $\Delta k = k_2 - k_1$. $f(x)$ is the structure function, and it equals 1 or -1 when$x$ falls in the positive or the negative domain, and f_1 is the Fourier coefficient; L is the length of the crystal; R is the reciprocal vector provided by the optical superlattice; γ_{eff1} (i = 1,2,3) are effective electro-optic coefficients as in Ref. 17. When $x \ll b_j$, the coupling equations will degenerate to the plane-wave approximation.

For a Gaussian beam, if we set the beam waist at (0,0,0), its vector potential A under the Davis procedure [18] is taken to have the form:

$$A_1(r) = \frac{iE_1}{k_1}\frac{1}{1+i\frac{2x}{k_1W_0^2}}\exp\left\{-\frac{r^2}{W_0^2\left(1+i\frac{2x}{k_1W_0^2}\right)}\right\}, \quad (6a)$$

$$A_2(r) = \frac{iE_2}{k_2}\frac{1}{1+i\frac{2x}{k_2W_0^2}}\exp\left\{-\frac{r^2}{W_0^2\left(1+i\frac{2x}{k_2W_0^2}\right)}\right\}, \quad (6b)$$

To simplify the calculation, we write the Gaussian beam vector potential in another form:

$$A(r) = A_1(r)\hat{e}_y + A_2(r)\hat{e}_z = A(r)[\alpha(r)\hat{e}_y + \beta(r)\hat{e}_z],$$

where the complex light amplitude $A(r)$ is expressed by a real-valued module u and phase ψ. α and β represent states of polarization across the yz section.

The x component of the angular momentum J of the Gaussian beam can be expressed by using the vector potential [14]:

$$\begin{aligned} J_x^{(1)} &\propto 2u^2\partial\psi/\partial\phi, \quad (7a) \\ J_x^{(2)} &\propto iu^2(\alpha\partial\alpha^*/\partial\phi + \beta\partial\beta^*/\partial\phi - c.c.), \quad (7b) \\ J_x^{(3)} &\propto ir\partial[u^2(\alpha\beta^* - \alpha^*\beta)]/\partial r, \quad (7c) \end{aligned}$$

where $J_x^{(1)}$ is the well-known OAM associated with the azimuthal gradient. $J_x^{(2)}$ and $J_x^{(3)}$ are associated with the distributions of state of the polarizations. In Ref. 14, a novel optical OAM associated with the curl of polarization, which is only related to $J_x^{(3)}$ and is independent of phase, is predicted. In that experiment, a pair of orthogonal base vectors was employed to generate radially-varying vector fields with hybrid SOPs that carry OAM.

Similarly, no azimuth angle factor ϕ is included in the vector potential of the Gaussian beam (Eq. (6)) in our scheme, so both $J_x^{(1)}$ and $J_x^{(2)}$ are zero. The remainder of the OAM, $J_x^{(3)}$, is determined by using Eq. (7c), which means it is only related to the radial distributions of the states of the polarization. Combining Eqs. (3), (6), and (7c), we arrive at

$$J_x^{(3)} \propto \frac{2i}{W_0^2}\left|\frac{E_1}{k_1}C_1\right|\left|\frac{E_2}{k_2}C_2\right|r^2\left\{D_1\exp\left(-\frac{r^2}{W_0^2}D_1\right) - D_2\exp\left(-\frac{r^2}{W_0^2}D_2\right)\right\}, \quad (8)$$

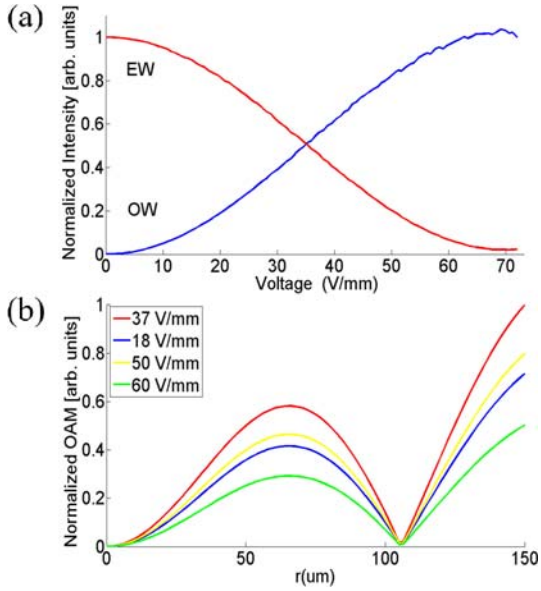

Fig. 2. (Color online) (a) Normalized extraordinary (EW) and ordinary wave (OW) intensities of the output beam vs the external electric field. The red and the blue lines represent the EW and the OW, respectively. (b) Normalized OAM of an output light beam passing through the PPLN controlled by using different external electric fields.

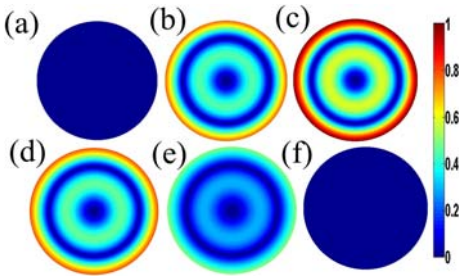

Fig. 3. (Color online) Spatial distribution of the OAM of the output beam for different E_0 with $\lambda = 632.8$ nm, $T = 298\ K$, $L = 2.5$ cm, $W_0 = 15\ \mu$m, $r_{out} = 150\ \mu$m: (a) $E_0 = 0$ V/mm, (b) $E_0 = 18$ V/mm, (c) $E_0 = 37$ V/mm, (d) $E_0 = 50$ V/mm, (e) $E_0 = 60$ V/mm, and (f) $E_0 = 74$ V/mm.

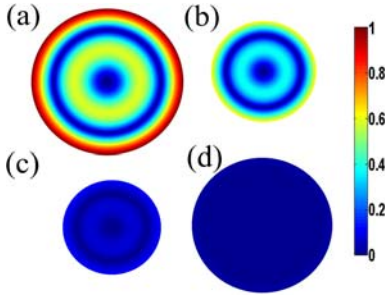

Fig. 4. (Color online) Spatial distribution of the OAM of the output beam for different W_0 with $\lambda = 632.8$ nm, $T = 298\ K$, $L = 2.5$ cm, and $E_0 = 37$ V/mm fixed: (a) $W_0 = 15$ um, $r_{out} = 150\ \mu$m, (b) $W_0 = 30$ um, $r_{out} = 80\ \mu$m, (c) $W_0 = 60$ um, $r_{out} = 70\ \mu$m, (d) $W_0 = 120$ um, $r_{out} = 120\ \mu$m.

where $C_j = (1+i2x/b_j)^{-1}$ $(j = 1{,}2)$, $D_1 = C_1 + C_2^*$, and $D_2 = D_1^*$. From Eq. (8), we find that the OAM varies with the external electric field, the beam waist and the length of crystal.

In the following, without loss of generality, we take a 2.5 cm PPLN with the period fixed as an example to analyze the above expression. The wavelength of the light is fixed at 632.8 nm. The refractive indices $n_1 = 2.2884$ and $n_2 = 2.2019$ are calculated from the Sellmeier equations for pure $LiNbO_3$ [19] at room temperature (298 K). To illustrate the influence of an external electric field on the OAM of light beam, we set the beam waist at 15 μm and take the initial condition as the incident light being an extraordinary wave ($g_1(0) = 0$, $g_2(0) = 1$).The coupling between ordinary and extraordinary light is controlled by using the external electric field. When the extraordinary light is launched into PPLN, the amplitude of the ordinary light is coupled out from it on the output surface of the crystal, as shown in Fig. 2(a). We can see that when the external electric field rises to 74 V/mm, the extraordinary wave can be absolutely transferred to ordinary light. For convenience, we define the maximum OAM when $E_0 = 37$ V /mm as the normalized value 1. Interesting phenomena are found in Fig. 2(b): (1) OAM is 0 at $r = 0$ and $r = 105\ \mu$m regardless of the value of the applied electric field because Eq. (8) is zero. (2) The distributional pattern of the OAM does not change, but the OAM value varies under different applied electric fields E_0.

Figure 3 shows the OAM distribution of the light under different applied electric fields, and it varies periodically with increasing external electric field. On the output surface of the crystal, the beam radius is about 150 μm. For every figure, J always reaches its maximum at the external ring. As is shown in Figs. 3(a) and (f), the OAM of the output beam is zero across the beam section because the output light is linearly polarized, corresponding to external electric fields of $E_0 = 0$ V/mm and 74 V/mm, respectively. Under the first condition ($E_0 = 0$ V/m), the output beam keeps its polarization without the effect of an external electric field. Under the second condition ($E_0 = 74$ V/mm), extraordinary light can be converted to ordinary light completely. Anyway, one of the two electric field components in Eq. (8) is zero, so J is null. Figures 3(b) – 3(e) show the OAM distributions when E_0 takes different voltages. The maximum J is reached when the intensity of the extraordinary wave equals that of the ordinary wave at $E_0 = 37$ V/mm in Fig. 3(c).

Not only the applied electric field but also the beam waist influences the OAM of the output beam. We assume incident extraordinary light and fix $E_0 = 37$ V/mm, $L = 2.5$ cm. The OAM distributions are shown in Figs. 4(a) – 4(d) with W_0 taken at 15 μm, 30 μm, 60 μm, and 120 μm and the radii of the output beams changing accordingly. The maximum OAM be-

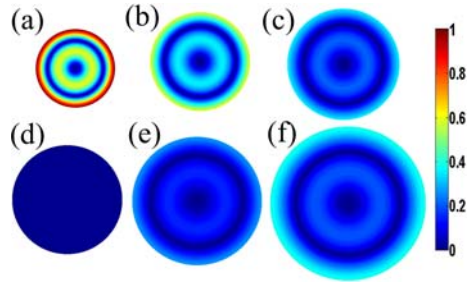

Fig. 5. (Color online) Spatial distribution of the OAM of the output beam for different crystal lengths L with $\lambda = 632.8$ nm, $T = 298$ K, $W_0 = 15$ μm, $E_0 = 37$ V/mm: (a) $L = 2.5$ cm, $r_{out} = 150$ μm, (b) $L = 3.4$ cm, $r_{out} = 200$ μm, (c) $L = 4.0$ cm, $r_{out} = 235$ μm, (d) $L = 5.0$ cm, $r_{out} = 290$ μm, (e) $L = 5.8$ cm, $r_{out} = 335$ μm, (e) $L = 6.6$ cm, $r_{out} = 400$ μm.

comes smaller with increasing of W_0. It will decrease to 0 when the waist becomes infinite because the focused Gaussian beams will degenerate to plane waves. Hence, we achieve spatial inhomogeneity of the polarization controlled by an external electric field, through which a continuous change in the OAM distribution can be manipulated.

We also investigated the OAM by selecting different lengths of the crystal. We set the initial condition so that the applied electric field is 37 V/mm and the beam waist radii is 15 μm. When the crystal becomes longer, the radii of the output beam becomes larger. The maximum value of the OAM in Figs. 5(a) – 5(f) are 1, 0.71, 0.35, 0, 0.27, and 0.41, corresponding to the different crystal lengths, respectively. We can obviously see that the high-value area of the OAM is concentrated in the external ring. Especially, when L is taken to be 5.0 cm, the extraordinary light is absolutely modulated to ordinary light, which means that the OAM is 0.

III. CONCLUSION

In conclusion, we systematically investigate the OAM behavior of a focused Gaussian beam after passing through an optical superlattice under the electro-optic effect. This work presents a new method to generate and manipulate the OAM of a Gaussian beam. The OAM can be tuned continually by changing the applied electric field. Other parameters like the beam waist and the crystal length are proved to be effective means to control the OAM of the beam. This method will find splendid application in optical tweezers to manipulate micro particles.

ACKNOWLEDGMENTS

This research was supported by the National Natural Science Foundation of China and NSAF (Contract No. 10876019), and the Shanghai Leading Academic Discipline Project (No. B201).

REFERENCES

[1] L. Allen, M. W. Beijersbergen, R. J. C. Spreeuw and J. P. Woerdman, Phys. Rev. A **45**, 8185 (1992).
[2] M. W. Beijersbergen, L. Allen, H. van der Veen and J. P. Woerdman, Opt. Commun. **96**, 123 (1993).
[3] M. W. Beijersbergen, R. P. C. Coewinkel, M. Kristensen and J. P. Woerdman, Opt. Commun. **112**, 321 (1994).
[4] V. Yu. Bazhenov, M. V. Vasnetsov and M. S. Soskin, JETP Lett. **52**, 429 (1990).
[5] G. Birner, A. Niv, V. Kleiner and E. Hasman, Opt. Lett. **27**, 1875 (2002).
[6] A. Mair, A. Vaziri, G. Weihs and A. Zeilinger, Nature **412**, 313 (2001).
[7] D. N. Neshev, T. J. Alexander, E. A. Ostrovskaya and Y. S. Kivshar, Phys. Rev. Lett. **92**, 123903 (2004).
[8] A. Ashkin, Opt. Lett. **11**, 288 (1986).
[9] J. T. Barreiro, T-C. Wei and P. G. Kwiat, Nat. Phys. **4**, 282 (2008).
[10] J. Leach, M. J. Padgett, S. M. Barnett, S. Franke-Arnold and J. Courtial, Phys. Rev. Lett. **88**, 257901 (2002).
[11] S. Sasaki and I. McNulty, Phys. Rev. Lett. **100**, 124801 (2008).
[12] R. Marchiano and J-L. Thomas, Phys. Rev. Lett. **101**, 064301 (2008).
[13] K. C. Wright, L. S. Leslie, A. Hansen and N. P. Bigelow, Phys. Rev. Lett. **102**, 030405 (2009).
[14] X. L. Wang, J. Chen, Y. Li, J. Ding, C. S. Guo and H. T. Wang, Phys. Rev. Lett. **105**, 253602 (2010).
[15] H. B. Tang, L. X. Chen and W. L. She, Opt. Express **18**, 25000 (2010).
[16] G. Xu, T. Ren, Y. Wang, Y. Zhu, S. Zhu and N. Ming, J. Opt. Soc. Am. B **20**, 360 (2003).
[17] W. She and W. Lee, Opt. Commun. **195**, 303 (2001).
[18] L. W. Davis, Phys. Rev. A **19**, 1177 (1979).
[19] M. V. Hobden and J. Warner, Phys. Lett. **22**, 243 (1966).